

## Refinement of 2-Amino-6-(4-methyl-1-piperazinyl)-4-(tricyclo[3.3.1.1<sup>3,7</sup>]dec-1-yl)-1,3,5-triazine at Three Different Temperatures using Image-Plate Data

ANASTASSIS PERRAKIS,<sup>†\*</sup> THOMAS R. SCHNEIDER,<sup>a</sup> EKATERINI ANTONIADOU-VYZAS,<sup>b</sup>  
ZBIGNIEW DAUTER<sup>a</sup> AND STAVROS J. HAMODRAKAS<sup>c</sup>

<sup>a</sup>European Molecular Biology Laboratory (EMBL), c/o DESY, Notkestrasse 85, 22603 Hamburg, Germany, <sup>b</sup>Department of Pharmaceutical Chemistry, University of Athens, Panepistimiopolis, Athens 157 01, Greece and <sup>c</sup>Department of Biochemistry, Cell and Molecular Biology and Genetics, University of Athens, Panepistimiopolis, Athens 157 01, Greece. E-mail: perrakis@nki.nl

(Received 24 July 1995; accepted 2 January 1996)

### Abstract

The structure of 2-amino-6-(4-methyl-1-piperazinyl)-4-(tricyclo[3.3.1.1<sup>3,7</sup>]dec-1-yl)-1,3,5-triazine was refined using data collected at three different temperatures [room temperature (293 K), 150 K and 85 K] with the use of an image-plate scanner in an attempt to study the effect of temperature on the disorder of the adamantyl group. It is demonstrated that the data collected with the rotation method and an image-plate scanner are of a high enough quality to be used for the refinement of small-molecule structures.

### 1. Introduction

The title compound has been synthesized as a possible dihydrofolate reductase [5,6,7,8-tetrahydrofolate: NADP<sup>+</sup> oxidoreductase (EC 1.5.1.3); DHFR] inhibitor. Its crystal structure has been solved and refined to an *R* value of 0.061 in space group *R*3, from diffractometer data (Hamodrakas, Hempel, Camerman, Ottensmeyer, Tsita, Antoniadou-Vyzas & Camerman, 1992). The adamantyl moiety was found to be disordered in the crystal structure, adopting two distinct conformations.

In the present work, an attempt has been made to investigate the effect of low temperatures on the disorder of the adamantyl group. With this structure as a model system, we also tried to explore further the possibility of routinely using image-plate data for the solution and refinement of small-molecule crystal structures (Grochowski, Serda, Wilson & Dauter, 1994).

### 2. Materials and methods

#### 2.1. Data collection

Crystals were obtained by evaporation from methanol as prismatic blocks. Data at 293 K were collected from a crystal of approximately 1.0 mm<sup>3</sup> in volume glued to the end of a glass capillary. Upon completion of the data collection, the same crystal was cooled to 150 K

with an Oxford Cryostream (Cosier & Glazer, 1986). A crystal of similar morphology and size was used for data collection at 85 K. This crystal was transferred into a perfluorinated polyether and picked up with a glass fibre (Kottke & Stalke, 1993). For all data collections, radiation from a molybdenum tube powered at 60 kV and 50 mA, monochromatized by pyrolytic graphite, was used. The instrumental set-up consisted of a MAR research image-plate scanner equipped with a single-axis  $\varphi$ -rotation motor. The scanner was controlled by a VAX 3100 workstation. For data collection at low temperature, the rotation axis was housed in a perspex box to avoid formation of ice on the sample. The rotation method (Arndt & Wonacott, 1977) was employed with the standard protocol for macromolecular X-ray data collection.

The limited dynamic range of the electronics controlling the image-plate scanner causes saturation effects for high-intensity reflections. For the parts of reciprocal space where overloaded reflections had occurred, data collection was repeated with a shorter exposure time to alleviate this problem. Simultaneously, the crystal-to-plate distance and the oscillation range per image were adjusted to achieve both higher accuracy and efficiency. The data-collection parameters are shown in Table 1. At room temperature, three data sets with different exposure times and crystal-to-plate distances were collected. For the low-temperature experiments, it was judged that two data sets were sufficient to record accurately the high-intensity terms.

The images were processed with the program *DENZO* (Otwinowski, 1993a). For the high-resolution data sets, both fully and partially recorded reflections were used. For the low-resolution data sets, only fully recorded observations were evaluated because, with a 10° oscillation range, the majority of reflections were fully recorded in a single rotation image. Integrated intensities from individual oscillation images were scaled on the basis of symmetry-related reflections and merged.

#### 2.2. Refinement

Using *SHELXL-93* (Sheldrick, 1993), the same protocol was employed for refinement of the structure

<sup>†</sup> Current address: Netherlands Cancer Institute (NKI) Department H2, Plesmanalaan 121, 1066 CX Amsterdam, The Netherlands.

Table 1. Summary of data collection

$$R(I) = \sum |I - \langle I \rangle| / \sum I, R(\sigma) = \sum \sigma(I) / \sum I.$$

	Room temperature			150 K		85 K		Picker Facs-1
	High	Medium	Low	High	Low	High	Low	
Space group	R3			R3		R3		R3
<i>a</i> = <i>b</i> (Å)	30.29 (7)			30.15 (3)		30.16 (6)		30.27 (2)
<i>c</i> (Å)	10.13 (3)			9.99 (1)		9.95 (1)		10.13 (1)
Volume (Å <sup>3</sup> )	8049			7864		7838		8044
Radiation source	Mo Kα			Mo Kα		Mo Kα		Cu Kα
Δφ (°)	3	5	10	3	6	3	6	
Exposure/image (s)	180	60	30	240	60	120	60	
Total φ (°)	180	180	180	99	102	126	102	
Distance (mm)	70	140	200	85	150	85	150	
Maximum resolution (Å)	0.9			0.9		0.9		0.9
Reflections measured	17 534			12 558		17 185		3023
Reflections expected	2572			2511		2503		2574
Unique reflections	2555			2506		2502		2292
Redundancy	6.9			5.1		6.9		1
Completeness (%)	99.3			99.8		100		89.1
<i>R</i> ( <i>I</i> ) (%)	1.9			1.5		2.2		n/a
<i>R</i> (σ) (%)	2.4			1.4		2.3		6.9
<i>I</i> /σ( <i>I</i> )	29.4			51.2		37.2		17.1

against  $F^2$  for all three image-plate data sets as well as for a new refinement of the diffractometer data (Hamodrakas *et al.*, 1992) for comparison purposes. The starting model for the refinements was the final model of Hamodrakas *et al.*, after removal of H atoms. Restrained anisotropic displacement parameters (*DELU* and *SIMU*) were employed from the start for all non-H atoms. Distance restraints describing the threefold symmetry of the disordered adamantyl group were applied. A free variable was refined to estimate the occupancies of the two modelled adamantyl conformations, whose sum was constrained to be unity. Ten initial cycles of full-matrix least-squares refinement were performed to adjust coordinates and temperature factors. Five more cycles were run using the weighting scheme recommended by *SHELXL-93* after the first run. All H atoms were added and refined in ten cycles using a 'riding' model with fixed distances and their temperature factors constrained to a value of 1.2 times the temperature factor of the respective parent atom.

The results of the refinement are summarized in Table 2 and Fig. 1.\*

### 3. Results and discussion

#### 3.1. Data collection

The  $R_{\text{merge}}$  on intensities for all symmetry-equivalent and multiply recorded reflections is remarkably low for all three image-plate data sets (Fig. 2). The strategies used in image-plate and diffractometer data collection differ in a number of parameters (Table 1), but are

\* Lists of structure factors, anisotropic thermal parameters, atom coordinates, bond lengths and bond angles have been deposited with the IUCr (Reference: LI5002). Copies may be obtained through The Managing Editor, International Union of Crystallography, 5 Abbey Square, Chester CH1 2HU, England.

the standard procedures used for both detector types. Despite the differences, the data resulting from the image-plate experiment are of a quality comparable to the diffractometer data and sufficient for accurate refinement of the molecular structure.

#### 3.2. Unit-cell determination

For intensity evaluation from an image-plate scanner, a number of parameters describing the crystal, its orientation and the scanner set-up are refined for every image to obtain a best fit between the calculated and predicted locations of the diffraction spots. Fitted parameters (including the unit-cell constants) usually vary slightly between successive images. In contrast to diffractometer measurements, the  $\theta$  angles are not

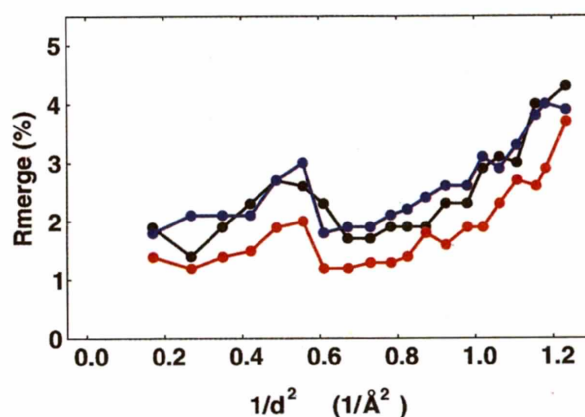


Fig. 1.  $R_1$  versus resolution.  $R_1$  is in % and the resolution in  $1/d^2$ . The broken black line corresponds to the room-temperature Picker Facs-1 data, the full black line to the room-temperature image-plate data, the red line to the 150 K image-plate data and the blue line to the 85 K image-plate data.

measured directly but are derived from the crystal-to-plate distance and the spot location on the image, giving rise to systematic errors. Thus, the precision of the unit-cell parameters derived from image-plate data collection is not as high as the corresponding parameters measured on a diffractometer, where they are estimated from directly measured  $2\theta$  angles.

Unit-cell parameters and their standard deviations were established from a post-refinement of the respective parameters as implemented in *SCALEPACK* (Otwinowski, 1993*b*). The cell parameters were post-refined independently for every rotation image and their mean value was then calculated, together with the e.s.d.'s. The unit-cell parameters at room temperature derived from the image-plate data display larger uncertainties than the corresponding values derived from the diffractometer, but are identical within errors. Upon cooling, the cell volume decreased by 0.21% at 150 K and 0.27% at 85 K. This is within the typical range for the size of the molecule (Lonsdale, 1972).

### 3.3. Adamantyl disorder

The disorder of the adamantyl moiety can be described by two discrete conformations (Fig. 3) at all three temperatures (Fig. 4). The torsion angles of the two adamantyl conformations with respect to the triazine ring do not differ significantly with varying temperature (Table 3). Owing to the threefold symmetry of the adamantyl group, the difference of  $\sim 180^\circ$  between the torsion angles of the 'A' and 'B' conformations is equivalent to a rotation around the C4–C9 bond by any integer multiple of  $60^\circ$ . Note that the estimated standard deviation for the angles derived from the diffractometer data is twice as high as for any of the image-plate data sets, reflecting the difference in data quality.

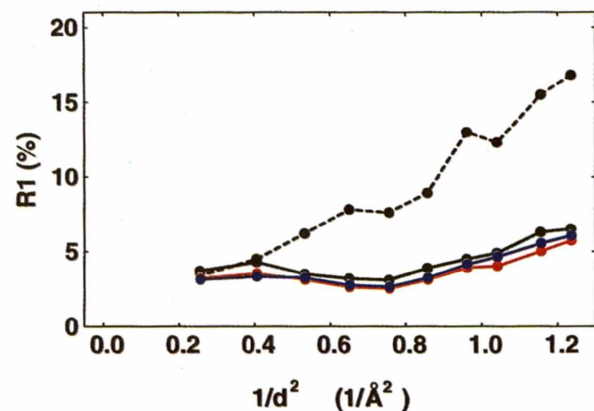


Fig. 2.  $R_{\text{merge}}$  versus resolution.  $R_{\text{merge}}$  is in % and the resolution in  $1/d^2$ . Black corresponds to room temperature, red to 150 K and blue to 85 K.

Table 2. Summary of refinement

Weight =  $1/\sigma^2(F_o^2) + \text{weight } A \times P^2 + \text{weight } B \times P$ , where  $P = (F_o^2 + 2F_c^2)/3$ ;  $wR2 = \sum w(F_o^2 - F_c^2)^2 / \sum w(F_o^2)^2$ ;  $R1 = \sum ||F_o| - |F_c|| / \sum |F_o|$ ; goodness of fit (GoF) =  $\sum w(F_o^2 - F_c^2)^2 / (n - p)^2$ , where  $n$  is the number of reflections and  $p$  is the total number of parameters. In the restrained GoF,  $\sum [w(yt - y)^2]$  (where  $y$  is the quantity being restrained and  $yt$  is its target value) is added to the numerator and the number of restraints is added to the denominator.

	Room temperature	150 K	85 K	Picker Fabs-1
Reflections used	2554	2506	2502	2292
Parameters	300	300	300	300
Restraints	632	626	626	632
Weight A	0.0619	0.0461	0.0474	0.0340
Weight B	4.364	7.939	10.748	17.788
Extinction	0.0028	0.0036	0.0017	0.0016
wR2 (%)	11.41	9.30	9.83	15.50
R1 (%)	4.08	3.57	3.68	7.56
R1( $F_o > 4\sigma F_o$ ) (%)	3.90	3.47	3.58	5.97
GoF	1.068	1.093	1.071	1.094
Restrained GoF	1.006	1.004	0.987	0.999
Mean e.s.d. (bonds) (Å)	0.0045	0.0033	0.0036	0.0049
Maximum e.s.d. (bonds) (Å)	0.0060	0.0050	0.0060	0.0070
Mean e.s.d. (angles) (°)	0.25	0.28	0.28	0.35
Maximum e.s.d. (angles) (°)	0.80	0.90	0.90	0.90

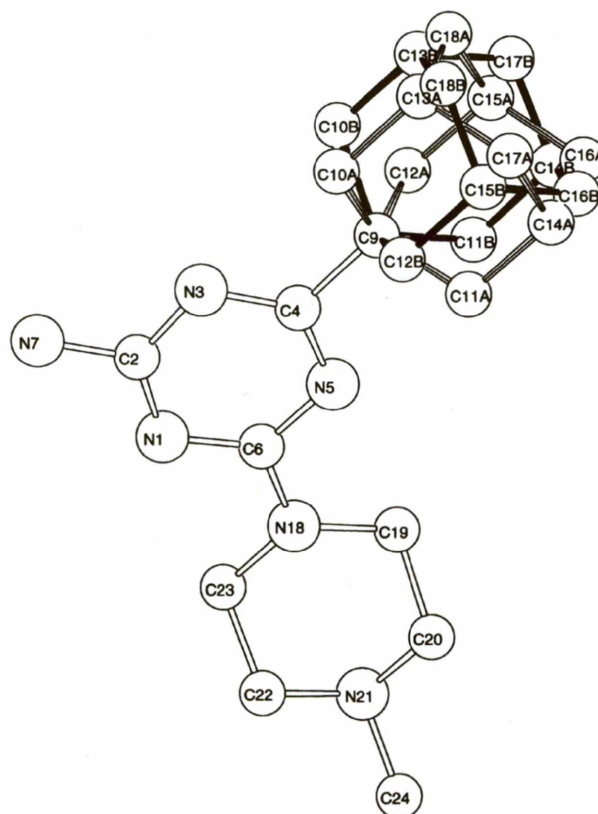


Fig. 3. Schematic representation of the title compound with the atomic numbering scheme.

With the assumption that the system is in thermodynamic equilibrium at 293 and 150 K, the energy differences corresponding to the relative occupancies of the A and B conformations [0.38 (2) and 0.37 (2)  $\text{kJ mol}^{-1}$ , respectively] are identical within errors. The fact that the occupancies at 150 and 85 K are identical within

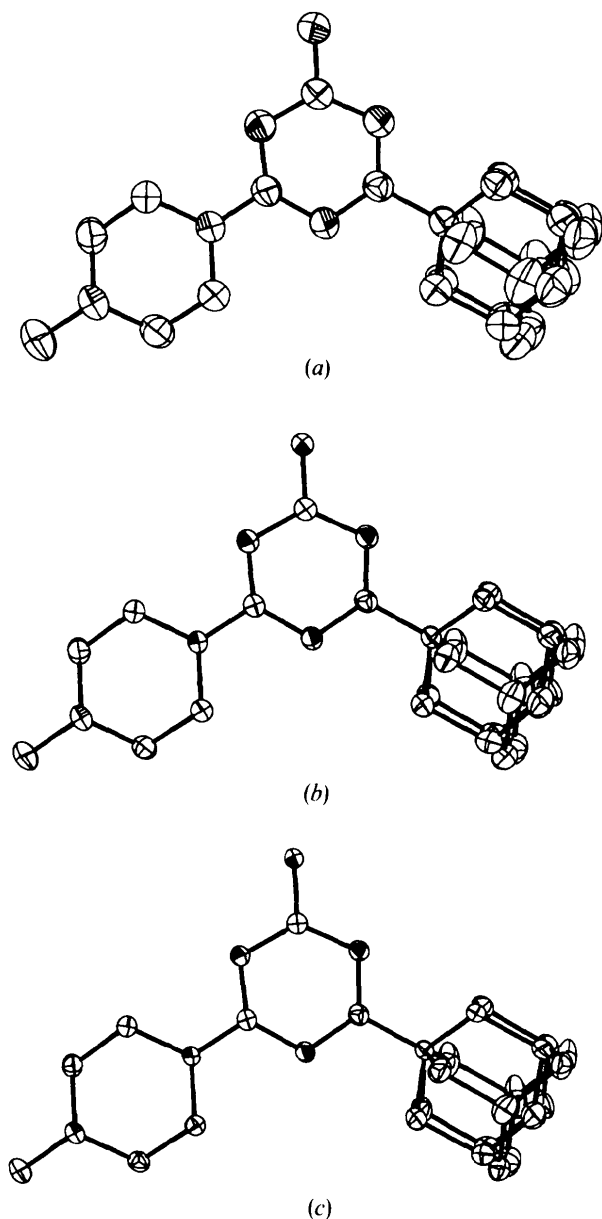


Fig. 4. 50% probability ellipsoids of the title compound for (a) room temperature, (b) 150 K and (c) 85 K. The decrease of the temperature factors is apparent. The positions of the two disordered adamantane conformations remain approximately the same at all temperatures. The figure was prepared using PLATON (Spek, 1992).

Table 3. Values for the torsion angles for  $N3-C4-C9-C11A$  and  $N3-C4-C9-C11B$  describing the two conformations of the adamantyl moiety with respect to the triazine ring ('A' and 'B') and  $C19-N8-C6-N5$  describing the orientation of the piperazine ring relative to the triazine ring

Torsion angles are given in degrees. Occupancies are given for the A conformation. Estimated standard deviations for angles and occupancies were obtained from full-matrix least-squares refinement and are given in parentheses. The corresponding energy differences were determined via Boltzmann's law.

	Room temperature	150 K	85 K	Picker Facs-1
$N3-C4-C9-C11A$	-102.3 (2)	-102.0 (2)	-102.0 (2)	-101.9 (4)
$N3-C4-C9-C11B$	83.0 (3)	84.0 (2)	84.2 (2)	83.4 (4)
$C19-N8-C6-N5$	-13.5 (2)	-14.2 (2)	-14.3 (2)	-13.6 (4)
Occupancy (%)	53.9 (2)	57.4 (2)	57.2 (2)	53.3 (4)
$\Delta E$ ( $\text{kJ mol}^{-1}$ )	0.38 (2)	0.37 (2)	[0.20(1)]	0.33 (4)

error indicates that there is an energy barrier between the two states that cannot be crossed at temperatures below 150 K. Therefore, the system cannot reach thermodynamic equilibrium and the derived energy difference between the two states becomes meaningless.

From this, the following picture for the disorder of the adamantyl emerges: (1) There are two possible conformations with a difference in energy of  $\sim 0.38 \text{ kJ mol}^{-1}$ . (2) The two conformations are related by a rotation of  $\sim 60^\circ$  around the  $C4-C9$  bond. (3) Above 150 K, thermal energy is sufficient for dynamical transitions across the energy barrier between the two conformations.

## References

- Arndt, U. W. & Wonacott, A. J. (1977). *The Rotation Method in Crystallography*, pp. 75-103. Amsterdam: North-Holland.
- Cosier, J. & Glazer, A. M. (1986). *J. Appl. Cryst.* **19**, 105-107.
- Grochowski, J., Serda, P., Wilson, K. S. & Dauter, Z. (1994). *J. Appl. Cryst.* **27**, 722-726.
- Hamodrakas, S. J., Hempel, A., Camerman, N., Ottensmeyer, F. P., Tsitsa, P., Antoniadou-Vyzas, E. & Camerman, A. (1992). *J. Cryst. Spectrosc. Res.* **22**, 607-614.
- Kottke, T. & Stalke, D. (1993). *J. Appl. Cryst.* **26**, 615-619.
- Lonsdale, K. (1972). *International Tables for X-ray Crystallography*, Vol. III, edited by C. H. MacGillavry & G. D. Rieck. Birmingham: The Kynoch Press. (Present distributor Kluwer Academic Publishers, Dordrecht.)
- Otwinowski, Z. (1993a). *DENZO: An Oscillation Data Processing Program for Macromolecular Crystallography*. Yale University, New Haven, USA.
- Otwinowski, Z. (1993b). *SCALEPACK: Software for the Scaling Together of Integrated Intensities Measured on a Number of Separate Diffraction Images*. Yale University, New Haven, USA.
- Sheldrick, G. M. (1993). *SHELXL-93, Program for the Refinement of Crystal Structures*. University of Göttingen, Germany.
- Spek, A. L. (1992). *PLATON-92*. University of Utrecht, The Netherlands.